Morroniside protects SK-N-SH human neuroblastoma cells against H_2O_2-induced damage

JING-XING ZHANG[1,2], RUI WANG[2], JIN XI[2], LIN SHEN[2], AN-YOU ZHU[1], QI QI[2], QI-YI WANG[2], LUN-JUN ZHANG[1], FENG-CHAO WANG[1], HE-ZUO LÜ[1,2] and JIAN-GUO HU[1,2]

[1]Department of Clinical Laboratory, The First Affiliated Hospital of Bengbu Medical College;
[2]Anhui Key Laboratory of Tissue Transplantation, Bengbu Medical College, Bengbu, Anhui 233004, P.R. China

Abstract. Oxidative stress-induced cell injury has been linked to the pathogenesis of neurodegenerative disorders such as spinal cord injury, Parkinson's disease, and multiple sclerosis. Morroniside is an antioxidant derived from the Chinese herb Shan-Zhu-Yu. The present study investigated the neuroprotective effect of morroniside against hydrogen peroxide (H_2O_2)-induced cell death in SK-N-SH human neuroblastoma cells. H_2O_2 increased cell apoptosis, as determined by flow cytometry and Hoechst 33342 staining. This effect was reversed by pretreatment with morroniside at concentrations of 1-100 μM. The increase in intracellular reactive oxygen species (ROS) generation and lipid peroxidation induced by H_2O_2 was also abrogated by morroniside. H_2O_2 induced a reduction in mitochondrial membrane potential, increased caspase-3 activity, and caused downregulation of B cell lymphoma-2 (Bcl-2) and upregulation of Bcl-2-associated X protein (Bax) expression. These effects were blocked by morroniside pretreatment. Thus, morroniside protects human neuroblastoma cells against oxidative damage by inhibiting ROS production while suppressing Bax and stimulating Bcl-2 expression, thereby blocking mitochondrial-mediated apoptosis. These results indicate that morroniside has therapeutic potential for the prevention and treatment of neurodegenerative diseases.

Introduction

Neurodegenerative disorders are characterized by loss or dysfunction of neurons in the central nervous system (1,2). Oxidative stress and consequent mitochondrial dysfunc-

tion contribute to the pathology of spinal cord injury (3,4), stroke (5,6), Parkinson's disease (7), and Alzheimer's disease (8) via production of reactive oxygen species (ROS), which include hydrogen peroxide (H_2O_2), superoxide, singlet oxygen, and the hydroxyl radical (9).

ROS play an important role in intracellular signal transduction and gene expression in cell survival and organism development (10). However, excess accumulation of ROS can damage proteins, DNA and cell membranes (11). ROS induce cell death via the mitochondrial apoptosis pathway (12). Neurons are thought to be more susceptible to ROS owing to increased oxidative metabolism and fewer antioxidative enzymes (13,14). Suppression of ROS generation and inhibition of apoptosis can therefore potentially prevent neurodegeneration.

Cornus officinalis is among the most commonly used Chinese medical herbs and has been used to treat kidney- and brain-related diseases (15). Its biological activities include antioxidant (16,17), anti-inflammatory (18) and antimicrobial (19) effects. Morroniside is the major active ingredient of *C. officinalis* extract (20) (Fig. 1) and has been shown to reduce blood glucose, mitigate cerebral ischemia-reperfusion injury, and modulate the immune response (21). However, little is known concerning the effects of morroniside on oxidative stress-induced cell damage.

Materials and methods

Cell culture and treatment. SK-N-SH human neuroblastoma cells (Type Culture Collection of the Chinese Academy of Sciences, Shanghai, China) were cultured in Dulbecco's modified Eagle's medium (DMEM) supplemented with 10% (v/v) fetal bovine serum, 100 U/ml penicillin/streptomycin (all from Invitrogen, Carlsbad, CA, USA) in plastic 25-cm^2 flasks at 37˚C and under 5% CO_2, 95% air. Culture medium was changed every other day and the cells were subcultured once attaining 70-80% confluency. Morroniside (Phytomarker Ltd., Tianjin, China) was dissolved in D-PBS (Invitrogen) and H_2O_2 (Sinopharm Chemical Reagent Co. Ltd., Shanghai, China) was dissolved in sterile distilled water. SK-N-SH cells were pretreated with different concentrations of morroniside for 24 h, followed by incubation with H_2O_2 (200-400 μM) for 24 h to induce injury.

Correspondence to: Professor Jian-Guo Hu or Professor He-Zuo Lü, Department of Clinical Laboratory, The First Affiliated Hospital of Bengbu Medical College, 287 Chang Huai Road, Bengbu, Anhui 233004, P.R. China
E-mail: jghu9200@163.com
E-mail: lhz233003@163.com

Cell viability assay. The viability of the cells was assessed by 3-(4,5-dimethylthiazol-2-yl)-2,5-diphenyltetrazolium bromide (MTT) assay. Briefly, SK-N-SH cells were plated into 96-well plates at the density of $5x10^3$ cells/well. Cells were preincubated with morroniside (1, 10 and 100 μM) for 24 h before 200 μM H_2O_2 was administered. After a 24-h incubation, 20 μl of a 5 mg/ml stock solution of MTT (Sigma, St. Louis, MO, USA) was added to the culture medium and incubated in the dark for 4 h at 37˚C to allow for formazan formation. Then MTT formazan crystals were dissolved in 100 μl dimethyl sulfoxide (DMSO; Sigma) and spectrophotometrically determined at an absorbance of 570 nm. The percentage of cell viability was measured by normalization of all values to the control group (=100%).

Morphological observation. SK-N-SH cells were seeded into 6-well plates at the density of $2x10^5$ cells/well. When cell confluency achieved 70-80%, the cells were pre-incubated with morroniside for 24 h before H_2O_2 (200 μM) was added to induce cell damage for another 24 h. The growth and morphological changes in each group were observed under an inverted phase contrast microscope.

Cytotoxicity assay. Lactate dehydrogenase (LDH) assay was used to assay H_2O_2-induced cytotoxicity. SK-N-SH cells were seed into 96-well plates at a density of $5x10^3$ cells/well. After cells were exposed to H_2O_2 (200 μM) for 24 h, a total of 120 μl of cell medium was collected for LDH analysis according to the manufacturer's protocol included in the cytotoxicity assay kit (Beyotime Biotechnology, Nantong, China). The absorbance of each group was read at 490 nm. Each group had five duplicate wells and the experiments were repeated at least three times. Data are expressed as the percentage of LDH release of the injury group (H_2O_2-induced group).

Apoptosis analysis. In order to determine whether morroniside protects against H_2O_2-induced apoptosis, Hoechst 33342 (Sigma), a fluorescent nuclear dye, was used to detect cell apoptosis by observing the cell morphology. Briefly, SK-N-SH cells were treated as described above and then washed with phosphate-buffered saline (PBS) and incubated with Hoechst 33342 (10 μg/ml in PBS; Sigma) for 15 min at 37˚C in the dark. The cells were washed with PBS, fixed with cold 4% paraformaldehyde for another 15 min in room temperature, washed with PBS again, and then examined by fluroescence microscopy. The percentage of apoptotic cells was calculated as the ratio of apoptotic cells to the total cells counted. At least 500 cells were counted from more than 3 random microscopic fields.

Moreover, in order to confirm the anti-apoptotic effect of morroniside, flow cytometry with Annexin V-FITC and propidium iodide (PI) double staining (Beyotime Biotechnology) was performed. After SK-N-SH cells were treated with H_2O_2 (200 μM), $5x10^5$ cells were collected and counted for Annexin V-FITC and PI double staining. Briefly, cells in different groups were washed three times with cold PBS and stained with Annexin V-FITC for 15 min in the dark. After cells were washed another three times, PI was added and the fluorescence of each group was immediately analyzed by flow cytometry.
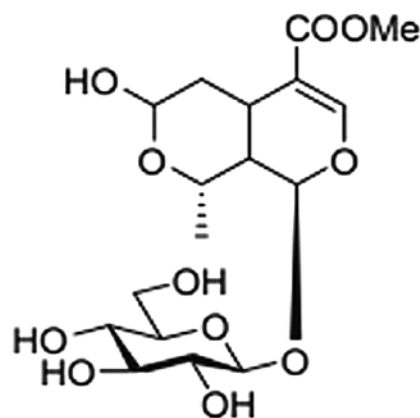

Figure 1. Chemical structure of morroniside.

Assessment of intracellular ROS production. For visualization and analysis of intracellular ROS, the oxidation sensitive probe DCFH-DA (Beyotime Biotechnology) was used. After the treatment of H_2O_2, SK-N-SH cells were exposed to 10 μM DCFH-DA for 20 min at 37˚C in the dark. The cells were washed with PBS for 3 times, and then DCF fluorescence was observed using fluorescence microscopy and quantified by fluorescence multi-well plate reader (BioTek, Highland Park, VT, USA) with an excitation wavelength of 488 nm and emission wavelength of 525 nm.

Measurement of intracellular superoxide anion production. Superoxide anion was detected with dihydroethidium probes. Cells were treated with 2 μM dihydroethidium (Beyotime Biotechnology) for 30 min at 37˚C in dim light after incubation with H_2O_2. Each well was washed with cold PBS and then DMEM to remove the remaining probes. Then cells were observed using fluorescence microscopy and the fluorescence intensity was quantified by a fluorescence multi-well plate reader.

Lipid peroxidation assay. Lipid peroxidation was monitored by measuring malondiadehyde (MDA; Beyotime Biotechnology), a stable end product of lipid peroxidation cascades using an MDA assay kit. SK-N-SH cells were washed with ice-cold PBS and then harvested with RIPA lysis buffer (Beyotime Biotechnology) after the treatment of H_2O_2. Cell homogenates were centrifuged at 16,000 x g at 4˚C for 10 min. The supernatant was used for MDA assay and protein determination. The total protein concentrations were measured using BCA Protein assay kit (Beyotime Biotechnology). For MDA measurement, 100 μl samples were added into a 15-ml tube followed by addition of 200 μl MDA working solution. The mixture was heated at 100˚C for 15 min, chilled to room temperature, and centrifuged at 1,000 x g for 10 min. Supernatants of 200 μl were transferred to 96-well plates, and the absorbance of each group was read at 532 nm.

Determination of activity of superoxide dismutase (SOD). Cellular SOD levels were determined using a Superoxide Dismutase assay kit (Jiancheng Bioengineering Institute, Nanjing, China). SK-N-SH cells were pretreated with different concentrations of morroniside for 24 h prior to exposure to

Table I. Sequences of the primers and PCR product sizes used in RT-PCR.

Gene	Primer	Sequence	Size (bp)
GAPDH	Sense	5'-AGAAGGCTGGGGCTCATTTG-3'	258
	Antisense	5'-AGGGGCCATCCACAGTCTTC-3'	
Bax	Sense	5'-CCAAGGTGCCGGAACTGA-3'	57
	Antisense	5'-CCCGGAGGAAGTCCAATGT-3'	
Bcl-2	Sense	5'-CATGTGTGTGGAGAGCGTCAAC-3'	187
	Antisense	5'-CTTCAGAGACAGCCAGGAGAAATC-3'	

GAPDH, glyceraldehyde 3-phosphate dehydrogenase; Bax, Bcl-2-associated X protein; Bcl-2, B cell lymphoma-2.

H_2O_2 (200 μM) for another 24 h. Cells were washed twice with ice-cold PBS and harvested in RIPA lysis buffer, and then total protein contents were determined with the BCA protein assay kit (Beyotime Biotechnology). Samples were collected and analyzed according to the manufacturer's instructions. SOD levels were normalized to the protein concentrations.

Monitoring mitochondrial membrane potential (MMP). SK-N-SH cells were treated with various dose of morroniside in a 12-well plate for 24 h before H_2O_2 (200 μM) for 24 h. A fluorescent dye JC-1 (Beyotime Biotechnology) was added to achieve final concentration of 10 μg/ml. Then cells were incubated for 30 min at 37°C in dim light. Cells were washed with PBS to remove the excess dye, and then images were captured using fluorescence microscopy within 30 min. For the JC-1 monomer, excitation wavelength was 514 nm and maximum emission wavelength was 529 nm. For the JC-1 polymer, the maximum excitation and emission wavelength were 585 and 590 nm, respectively.

Measurement of caspase-3 activity. Activity of caspase-3 was measured with a commercial caspase-3 activity assay kit (Beyotime Biotechnology), using Ac-DEVD-pNA as the specific substrate. The cell pellets were lysed on ice in lysis buffer for 15 min, and then the lysate was centrifuged at 20,000 x g for 10 min at 4°C. Supernatant of 10 μl was collected and incubated with 10 μl Ac-DEVD-pNA (2 mM) at 37°C for another 1-2 h in the dark. The absorbance values were measured with a spectrofluorometer at 405 nm and were corrected as protein content in the lysate. Protein concentration was determined by Bradford protein assay kit (Beyotime Biotechnology) according to the manufacturer's instructions.

Reverse transcription-polymerase chain reaction (RT-PCR). The mRNA expression levels of B cell lymphoma-2 (Bcl-2) and Bcl-2-associated X protein (Bax) were determined by RT-PCR. Briefly, SK-N-SH cells were treated as mentioned above, and the total RNA of each group was extracted using TRIzol agent (Invitrogen) according to the manufacturer's instructions. Two micrograms of total RNA was first reverse transcribed into cDNA, and then routine PCR was performed as previously described (22). Glyceraldehyde 3-phosphate dehydrogenase (GAPDH) was used as an internal control and products were analyzed on 1% agarose gel. ImageJ software

(NIH, Bethesda, MD, USA) was used to quantify the optical density value of each band. The sequences of specific primers (Sangon Biotech Inc., Shanghai, China) used for RT-PCR are listed in Table I.

Western blot analysis. Cells were collected at 24 h after exposure to H_2O_2. In order to detect the expression of Bcl-2 and Bax, SK-N-SH cells were washed with PBS and lysed using a lysis buffer for 30 min on ice. Lysates were centrifuged at 16,000 x g for 10 min at 4°C, and the supernatant was saved for the total protein determination. Protein concentrations were determined using a commercially available BCA protein assay kit (Beyotime Biotechnology). For western blot analysis, equivalent amounts of protein of each sample (20 μg) were electrophoresed using sodium dodecyl sulfate-polyacrylamide gel electrophoresis (SDS-PAGE), and transferred to polyvinylidene difluoride membranes (Millipore, Bedford, MA, USA). After the membranes were blocked with 5% non-fat dry milk in Tris-buffered saline (TBS) for 1 h at room temperature, primary antibodies (in TBST-5% BSA) against Bcl-2 (1:2,000; 12789-1-AP) and Bax (1:5,000; 60267-1-Ig) (both from ProteinTech Group Inc, Chicago, IL, USA) were added and incubated overnight at 4°C for determining signal transduction events. The membranes were rinsed three times with TBST and incubated with an appropriate HRP-conjugated secondary antibody (1:2,000; #04-15-06 and #04-18-06) (both from KPL, Gaithersburg, MD, USA) for 1 h at 37°C. An ECL kit (Millipore) was used to visualize membrane immunoreactivity. Quantification was performed using a computerized imaging program Quantity One (Bio-Rad, Hercules, CA, USA).

Statistical analysis. All data are presented as mean ± standard deviation of the mean (SD). Statistical analyses were performed by one-way analysis of variance (ANOVA) with post hoc Tukey's t-test to determine statistical significance. A value of $P < 0.05$ was considered to indicated statistically significant differences.

Results

Morroniside attenuates H_2O_2-induced cell death. H_2O_2-induced cell injury was evaluated using the MTT assay. H_2O_2 reduced cell viability in a dose- and time-dependent manner, with a survival rate of 50% after 24 h in the presence
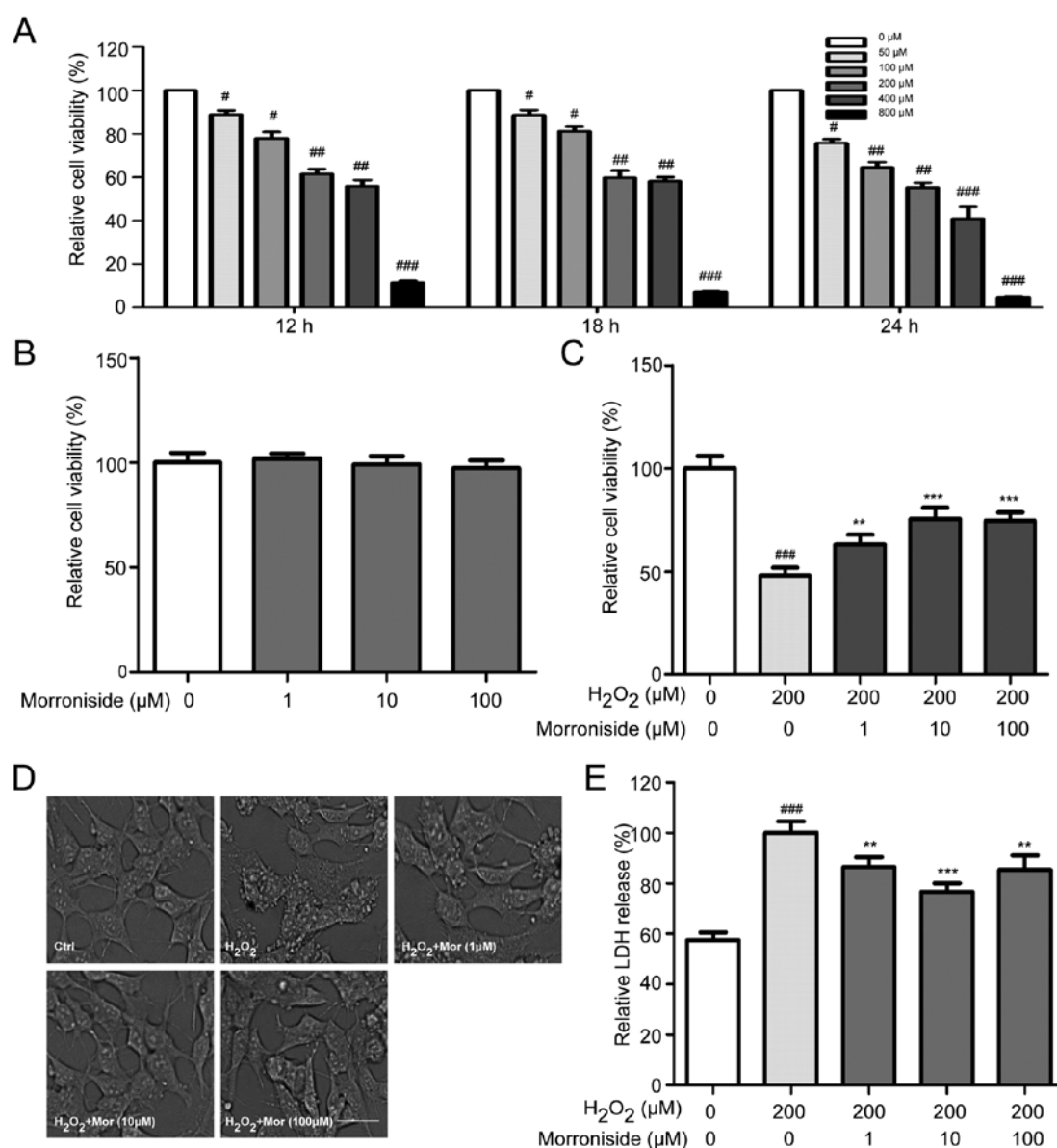
Figure 2. (A) Effects of H_2O_2 on SK-N-SH cell viability. Cell viability was reduced in a dose- and time-dependent manner by treatment with H_2O_2 (200 μM for 24). (B) Effects of morroniside on SK-N-SH cell viability. Morroniside treatment did not affect cell viability at concentrations of 1, 10 and 100 μM. (C) Effects of morroniside on H_2O_2-induced SK-N-SH cell death. Pretreatment with morroniside (1-100 μM) for 24 h restored viability in cells exposed to H_2O_2 (200 μM) in a dose-dependent manner. (D) Morroniside inhibits morphological changes resulting from H_2O_2 treatment. Scale bar, 20 μM. (E) Morroniside suppresses H_2O_2-induced lactate dehydrogenase (LDH) release in SK-N-SH cells. Cells were pretreated with indicated concentrations of morroniside (1-100 μM) for 24 h following treatment with 200 μM H_2O_2 or no treatment for 24 h. LDH activity in the medium was measured. Data represent mean ± SD (n=3). [#]P<0.05, [##]P<0.01 and [###]P<0.001 vs. control group; [**]P<0.01 and [***]P<0.001 vs. H_2O_2-treated group.

of 200 μM H_2O_2 relative to the untreated controls (Fig. 2A). Cells were treated with various concentrations of morroniside for 24 h to determine whether the H_2O_2-induced decrease in viability would be mitigated. Morroniside had no effect on the survival of SK-N-SH cells that were not treated with H_2O_2 (Fig. 2B). However, pretreatment with morroniside attenuated the H_2O_2-induced decrease in cell survival in a dose-dependent manner, with the greatest effect observed at 10 μM (Fig. 2C).

Morroniside reverses H_2O_2-induced morphological changes. SK-N-SH cells treated for 24 h with 200 μM H_2O_2 showed morphological changes including loss of cell projections;

a round, swollen, or shrunken cell body; and aggregation. These changes were blocked by pretreatment with morroniside (Fig. 2D).

Morroniside inhibits H_2O_2-induced LDH release. The LDH release assay showed that H_2O_2 increased LDH activity in the supernatant of the SK-N-SH cell cultures relative to the control group. This effect was suppressed upon treatment with 1, 10 and 100 μM morroniside (P<0.05) (Fig. 2E).

Morroniside protects SK-N-SH cells from H_2O_2-induced apoptosis. We investigated whether the H_2O_2-induced decrease in SK-N-SH cell survival was due to apoptosis by Hoechst 33342
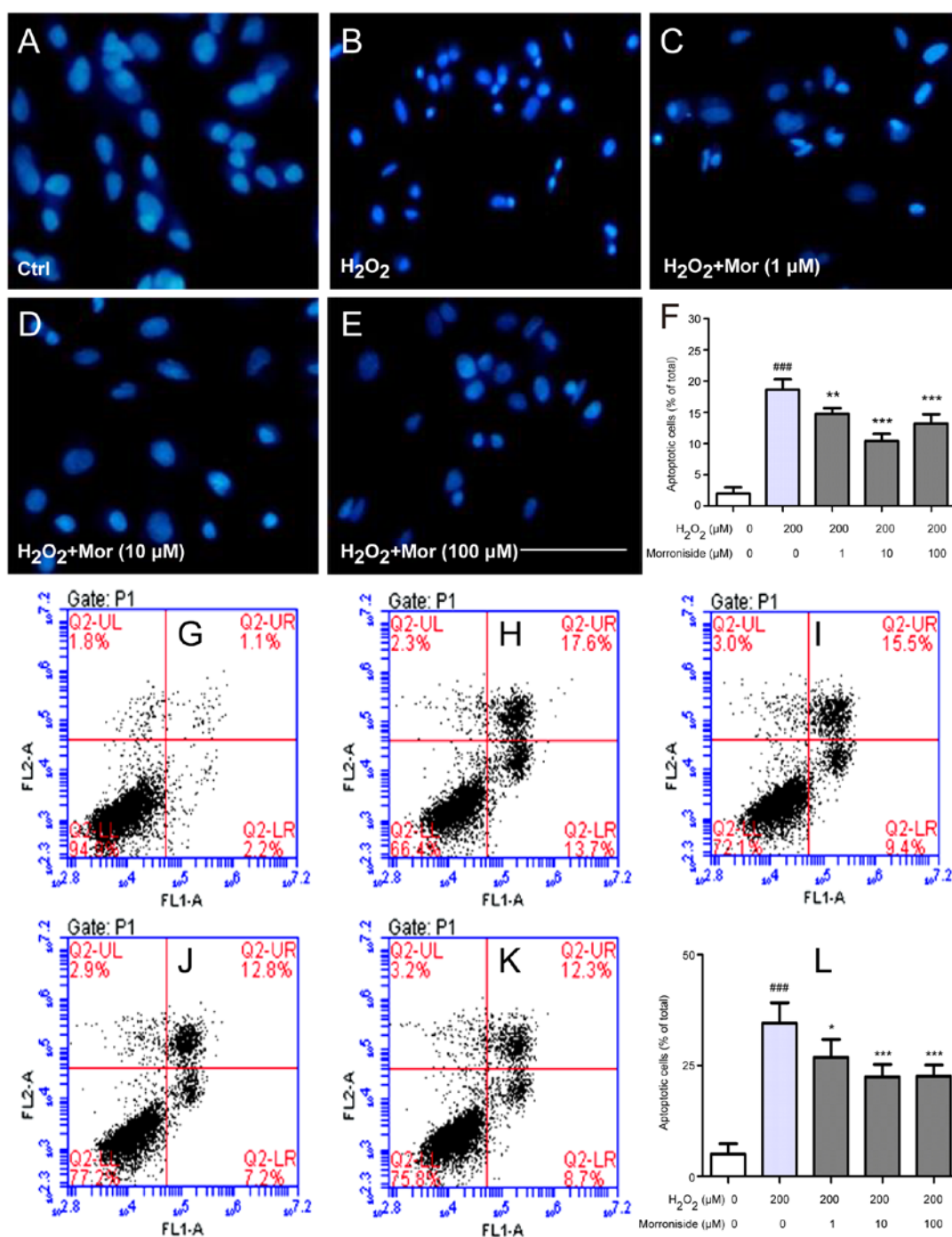
Figure 3. Morroniside blocks H_2O_2-induced apoptosis of SK-N-SH cells. Apoptotic nuclei were visualized by Hoechst 33342 staining. (A) Untreated cells with normal nuclei. (B) Cells exposed to 200 μM H_2O_2 with condensed nuclei. (C-E) Cells pretreated with morroniside at concentrations of (C) 1 μM, (D) 10 μM and (E) 100 μM for 24 h showed reduced sensitivity to the effects of H_2O_2, as evidenced by fewer cells with condensed nuclei. Scale bar, 20 μM. (G-K) Annexin V/ propidium iodide (PI) double-staining was used to confirm apoptosis in SK-N-SH cells. Few cells positive for Annexin V/PI staining were detected in the control group (G), while H_2O_2 (200 μM) treatment increased the percentage of Annexin V^+/PI^+ cells (H). Preincubation with (I) 1 μM, (J) 10 μM and (K) 100 μM morroniside for 24 h inhibited H_2O_2-induced apoptosis. Quantitative analyses are shown in panels (F and L). Data represent mean ± SD of three independent experiments. [###]P<0.001 vs. control group; [*]P<0.01, [**]P<0.01 and [***]P<0.001 vs. injury group.

and Annexin V/PI staining. Control cells stained with Hoechst 33342 had large, oval-shaped nuclei (Fig. 3A). H_2O_2 (200 μM) treatment increased the fraction of cells with condensed or fragmented nuclei (18.60±1.67 vs. 2.00±1.00%; P<0.01) (Fig. 3B and F). These defects were rescued by pretreatment with morroniside (1, 10 and 100 μM), which reduced the fraction of apoptotic cells (14.80±0.84,

10.40±1.14 and 13.20±1.48%, respectively vs. 18.60±1.67%; P<0.01) (Fig. 3C-F). Consistent with these findings, there were few cells positive for Annexin V/PI staining detected in the control group (Fig. 3G). H_2O_2 (200 μM) treatment increased the percentage of Annexin V^+/PI^+ cells (34.58±4.59 vs. 4.96±2.44%; P<0.001) (Fig. 3H and L), which was reduced by morroniside (1, 10 and 100 μM) treatment (26.86±4.05, 22.42±2.81
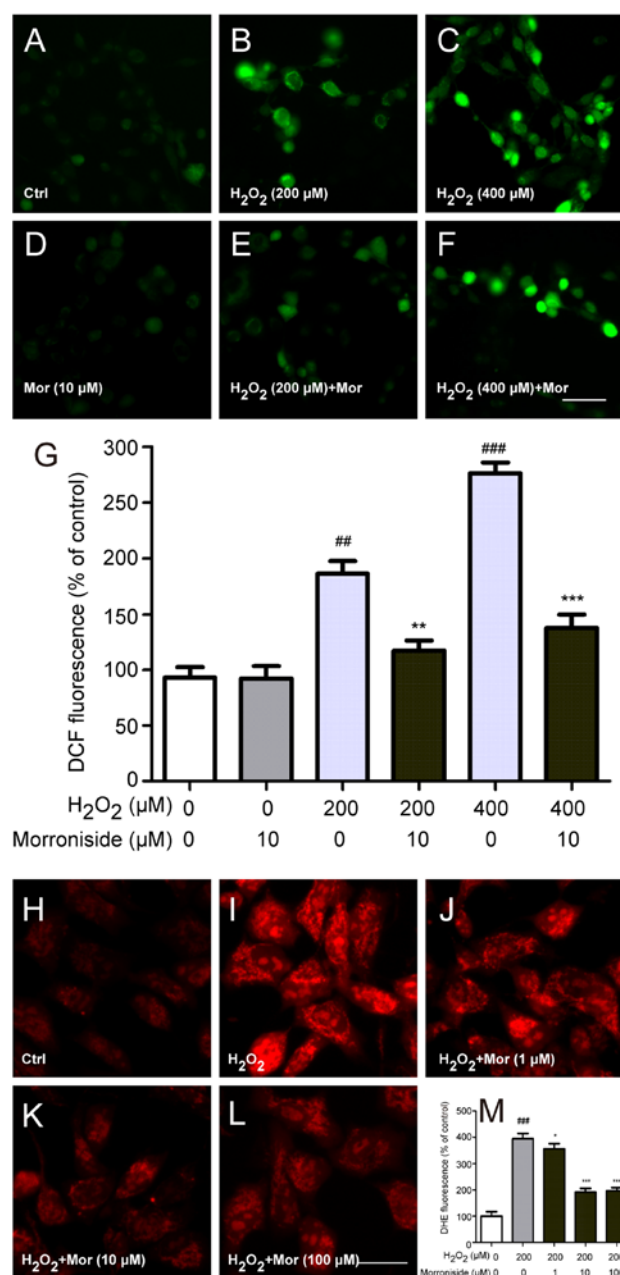
Figure 4. Morroniside attenuates H$_2$O$_2$-induced accumulation of intracellular reactive oxygen species (ROS) in SK-N-SH cells. Cells were pretreated with (D-F) 10 μM morroniside for 24 h followed by (B and E) 200 μM or (C and F) 400 μM H$_2$O$_2$ for 24 h. Untreated control cells are shown in (A). ROS levels were increased in a dose-dependent manner by treatment with (B) 200 μM and (C) 400 μM H$_2$O$_2$. The increase was abolished by pretreatment with 10 μM morroniside (E and F). Intracellular superoxide anion levels were measured by dihydroethidium staining. Compared to the control (H), H$_2$O$_2$ (200 μM) increased superoxide anion production (I), an effect that was reversed by pretreatment with (J) 1 μM, (K) 10 μM and (L) 100 μM morroniside. Quantitative analyses are shown (G and M). Data represent mean ± SD of three independent experiments. $^{\#\#}$P<0.01 and $^{\#\#\#}$P<0.001 vs. control group; *P<0.01, **P<0.01 and ***P<0.001 vs. injury group. Scale bars: (F) 50 μM and (L) 20 μM.

and 22.62±2.48%, respectively vs. 34.58±4.59%; P<0.05) (Fig. 3I-L).

Morroniside inhibits H$_2$O$_2$-induced elevation in intracellular ROS level. Intracellular ROS levels were detected
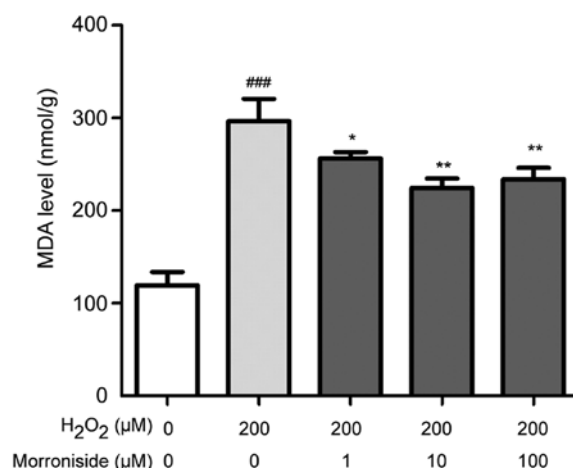

Figure 5. Effect of morroniside on H$_2$O$_2$-induced lipid oxidation. Cells were pretreated with indicated concentrations of morroniside for 24 h followed by 200 μM H$_2$O$_2$ for 24 h. Data represent mean ± SD of three independent experiments. $^{\#\#\#}$P<0.001 vs. control group; *P<0.01 and **P<0.01 vs. injury group.
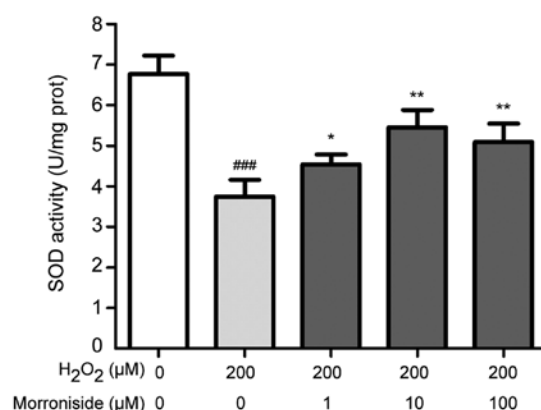

Figure 6. Morroniside blocks the H$_2$O$_2$-induced decrease in superoxide dismutase (SOD) level in SK-N-SH cells. Cells were pre-incubated with 1, 10 or 100 μM morroniside for 24 h followed by H$_2$O$_2$ for 24 h. Data represent mean ± SD of three independent experiments. $^{\#\#\#}$P<0.001 vs. control group; *P<0.01 and **P<0.01 vs. injury group.

with 2,7'-dichlorofluorescein (DCF) diacetate. SK-N-SH cells exposed to 200 and 400 μM H$_2$O$_2$ for 24 h showed dose-dependent increases in intracellular DCF fluorescence (P<0.01) (Fig. 4A-C and G), indicating that ROS levels were elevated. However, 10 μM morroniside pretreatment abrogated these increases in fluorescence intensity compared to the H$_2$O$_2$-treated groups (P<0.01) (Fig. 4E-G), suggesting a protective effect against H$_2$O$_2$-induced free radical formation.

Superoxide anion is a type of ROS that is associated with oxidative stress. To determine whether it is involved in H$_2$O$_2$-induced cytotoxicity, we measured intracellular superoxide anion levels with the dihydroethidium probe (Fig. 4H-M). The fluorescence intensity of SK-N-SH cells increased markedly after incubation for 24 h with H$_2$O$_2$ (P<0.001) (Fig. 4I and M). However, pretreatment with 1, 10 and 100 μM morroniside significantly reduced intracellular superoxide anion levels.

Morroniside suppresses H$_2$O$_2$-induced lipid peroxidation. Lipid peroxidation levels were monitored by detecting the
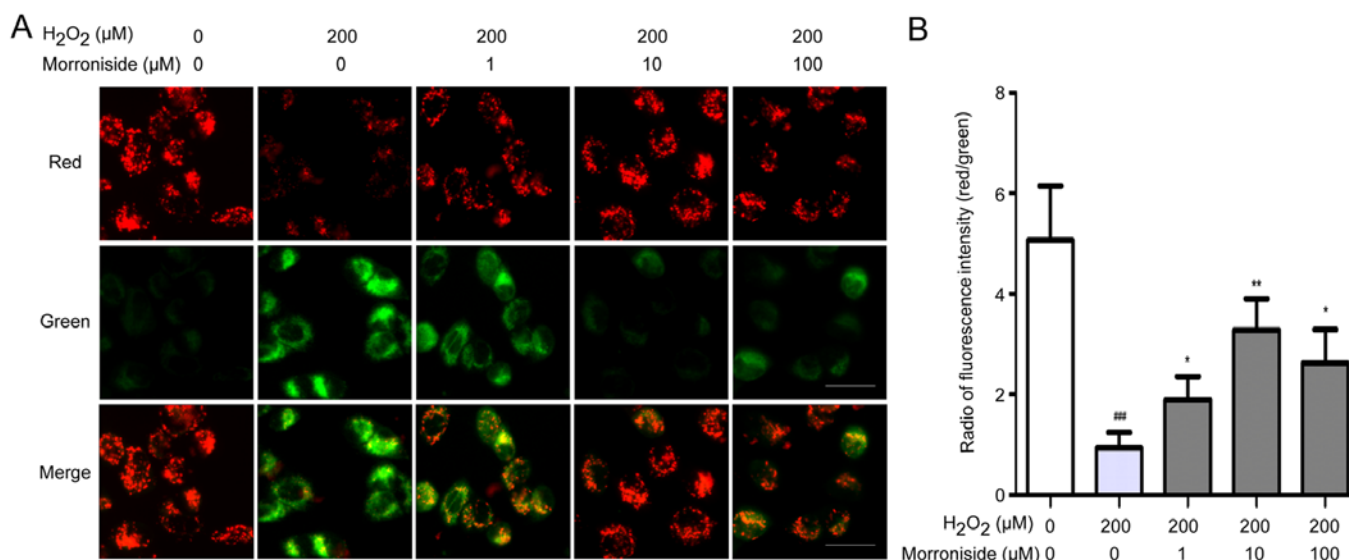
Figure 7. Inhibition of H_2O_2-induced reduction in mitochondrial membrane potential (MMP) by morroniside. (A and B) Cells were pretreated with the indicated concentrations of morroniside followed by 200 μM H_2O_2. The decrease in MMP was quantified with JC-1 staining and fluorescence microscopy. Scale bar, 20 μM.
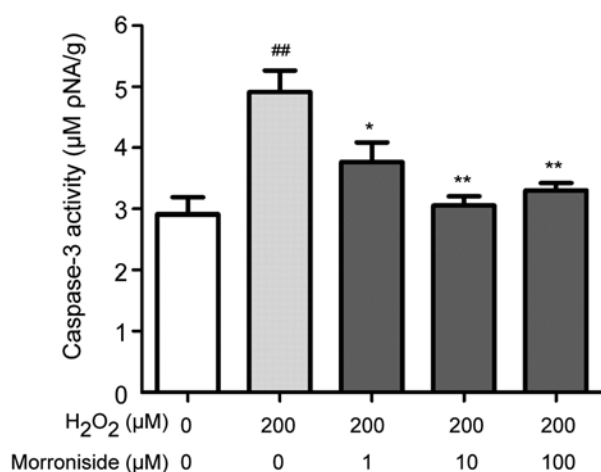

Figure 8. Effect of morroniside on caspase-3 activity. Cells were pretreated with indicated concentrations of morroniside for 24 h followed by H_2O_2 for 24 h. Data represent mean ± SD of four independent experiments. ##$P<0.01$ vs. control group; *$P<0.01$ and **$P<0.01$ vs. injury group.

stable end products of lipid peroxidation using an MDA assay kit. Under normal conditions, cellular MDA content was ~119.47±14.14 nmol/g protein (Fig. 5). In cells treated with 200 μM H_2O_2 for 24 h, the level was increased to 296.28±24.25 nmol/g protein ($P<0.001$). However, pretreatment with 1, 10 and 100 μM morroniside reduced MDA levels to 256.26±6.70, 223.63±12.47 and 224.35±10.18 nmol/g protein, respectively ($P<0.05$).

Morroniside inhibits H_2O_2-induced SOD depletion. To investigate the antioxidant properties of morroniside, we measured intracellular levels of SOD. Treatment with 200 μM H_2O_2 for 24 h reduced intracellular SOD levels from 6.77±0.45 to 3.74±0.41 U/mg ($P<0.001$). This was reversed by morroniside pretreatment at concentrations ranging from 1 to 100 μM; for

example, a concentration of 10 μM enhanced SOD level by over 45% relative to the H_2O_2-treated group (Fig. 6).

Morroniside suppresses H_2O_2-induced decreases in MMP. We investigated whether morroniside could suppress the H_2O_2-induced decrease in MMP using JC-1 dye. SK-N-SH cells treated with 200 μM H_2O_2 for 24 h showed an obvious decrease in MMP, as evidenced by a decrease in the ratio of red to green fluorescence (Fig. 7). This effect was mitigated by treatment with morroniside, most obviously at a concentration of 10 μM.

Morroniside inhibits H_2O_2-induced caspase-3 level. Caspase-3 is a key protein in the regulation of apoptosis. SK-N-SH cells treated with 200 μM H_2O_2 for 24 h showed a nearly 2-fold increase in the caspase-3 level relative to the control cells ($P<0.01$) (Fig. 8). Pretreatment with morroniside (1, 10 and 100 μM) suppressed the H_2O_2-induced upregulation of caspase-3 (3.77±0.31, 3.05±0.16 and 3.31±0.12 μM pNA/g, respectively vs. 4.91±0.36 μM pNA/g; $P<0.05$).

Morroniside modulates expression of apoptosis-related proteins. The expression levels of the apoptosis-related genes Bcl-2 and Bax were altered in the SK-N-SH cells by H_2O_2 administration; the Bcl-2 mRNA level was downregulated while that of Bax was upregulated (Fig. 9A-C). These changes were abolished by pretreatment with 1-100 μM morroniside. Similarly, western blot analysis revealed that H_2O_2 (200 μM) decreased the Bcl-2 level ($P<0.001$) and increased that of Bax ($P<0.01$) after 24 h (Fig. 9D-F). However, pretreatment with 1, 10 and 100 μM morroniside restored Bcl-2 and Bax expression levels compared to these levels in the H_2O_2-induced group.

Discussion

Oxidative stress caused by ROS is implicated in the pathogenesis of most chronic diseases (23,24). ROS accumulation
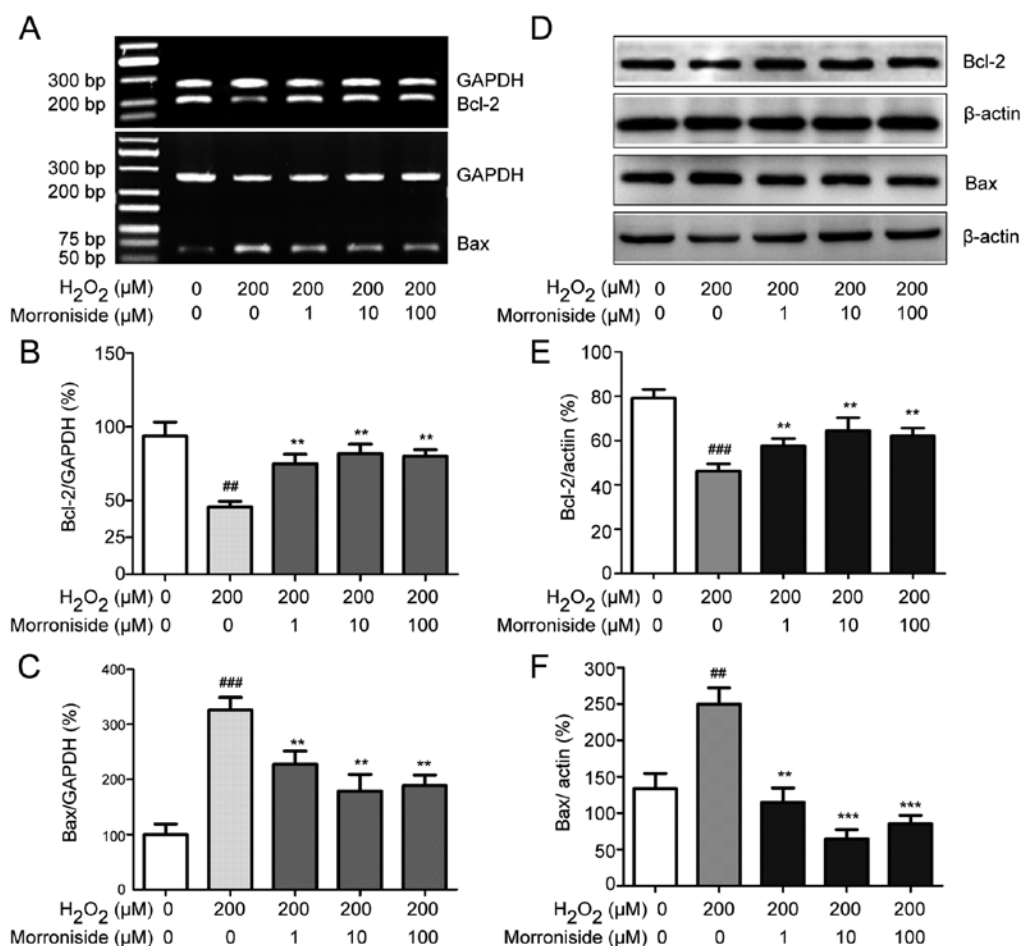
Figure 9. Effect of morroniside on the expression of apoptosis-related proteins. Cells were pretreated with the indicated concentrations of morroniside for 24 h followed by H$_2$O$_2$ for 24 h. Bcl-2 and Bax expression was evaluated by (A-C) RT-PCR and (D-F) western blotting. Values represent mean ± SD of three independent experiments. $^{\#\#}$P<0.01 and $^{\#\#\#}$P<0.001 vs. the control group; **P<0.01 and ***P<0.001 vs. the injury group.

results in cellular damage (5). Loss of neurons due to oxidative stress plays a key role in the development of cerebrovascular and/or neurodegenerative diseases (1,8,25). Neurons are thought to be more susceptible to oxidative damage than other cell types due to their high oxygen consumption and low antioxidant capabilities (26). In the present study, we found that H$_2$O$_2$, a freely diffusible ROS, induced apoptosis in the human neuroblastoma SK-N-SH cells.

Usually, antioxidants, especially those derived from natural sources, have many therapeutic applications (27,28). Morroniside is a constituent of *C. officinalis*, a traditional Chinese medicine (29), and has demonstrated protective effects against cerebral ischemic damage (15), indicating a potential role of morroniside on restoring injured neurons. However, little is known concerning the underlying mechanisms. In this study, we investigated the neuroprotective role of morroniside in SK-N-SH cells treated with H$_2$O$_2$.

Exposure of cells to exogenous H$_2$O$_2$ can induce ROS overproduction (30), leading to peroxidation of membrane lipids and disruption of cellular integrity (31). The present study showed that pretreatment with morroniside reversed H$_2$O$_2$-induced apoptosis by blocking ROS production.

SOD is a component of the antioxidant machinery in neurons (32). In most situations, ROS produced through

metabolic processes are quenched by intracellular defense systems, including SOD (33). Previous studies have shown that depletion of cellular glutathione leads to accumulation of ROS and mitochondrial dysfunction (34). We found here that morroniside treatment increased SOD activity in the SK-N-SH cells, which prevented ROS accumulation. Thus, we propose that the cytoprotective effects of morroniside are associated with its antioxidant capacity, for which, antioxidants such as glutathione or SOD are indispensable.

Overproduction of ROS disrupts the intracellular redox equilibrium, resulting in apoptosis (35). ROS target mitochondrial membrane proteins, leading to activation of the mitochondrial permeability transition pore, which decreases the MMP (36) and releases cytochrome *c* into the cytosol, where it binds to apoptotic protease activating factor 1 and forms the apoptosome, which activates pro-apoptotic caspases (37). Indeed, we observed that H$_2$O$_2$ treatment reduced the MMP and activated the pro-apoptotic protein caspase-3. These effects were blocked by pretreatment with morroniside, suggesting that morroniside exerts protective effects by blocking the mitochondrial apoptotic pathway.

H$_2$O$_2$ has been reported to modulate the levels of Bcl-2 and Bax, two genes associated with mitochondrial apoptosis, in various cell types including cortical neurons (30), endothelial

cells (38), and HT22 cells (39), specifically by suppressing Bcl-2 and stimulating Bax expression (30). This was observed in our study at both the mRNA and protein levels following administration of H_2O_2 for 24 h. Moreover, morroniside treatment reversed the changes in Bcl-2 and Bax expression induced by H_2O_2. The pro-apoptotic protein Bax is activated during apoptosis, and its relocation from the cytoplasm to the mitochondrial outer membrane leads to formation of the mitochondrial permeability transition pore and downstream events. Bax accumulated in the mitochondrial outer membrane binds to the anti-apoptotic protein Bcl-2 and maintains it in an inactive state (37). Bcl-2 also acts as an antioxidant by suppressing ROS levels and the mitochondrial apoptosis pathway (40). Taken together, these findings suggest that morroniside blocks mitochondrial apoptosis via modulation of Bcl-2 and Bax expression.

In conclusion, in the present study, morroniside was found to protect against H_2O_2-induced oxidative damage in SK-N-SH neuronal cells. This effect was mediated by inhibition of ROS-induced oxidative stress as well as suppressing and stimulating Bax and Bcl-2 expression, respectively, leading to inhibition of the mitochondrial apoptotic pathway. Thus, morroniside can potentially be used for the prevention and treatment of neurodegenerative diseases.

Acknowledgements

References

1. Destée A, Mutez E, Kreisler A, Vanbesien-Maillot C and Chartier-Harlin MC: Parkinson disease: Genetics and neuronal death. Rev Neurol (Paris) 165: F80-F85, 2009 (In French).
2. Zeineddine R and Yerbury JJ: The role of macropinocytosis in the propagation of protein aggregation associated with neurodegenerative diseases. Front Physiol 6: 277, 2015.
3. Jia Z, Zhu H, Li J, Wang X, Misra H and Li Y: Oxidative stress in spinal cord injury and antioxidant-based intervention. Spinal Cord 50: 264-274, 2012.
4. Bains M and Hall ED: Antioxidant therapies in traumatic brain and spinal cord injury. Biochim Biophys Acta 1822: 675-684, 2012.
5. Rodrigo R, Fernández-Gajardo R, Gutiérrez R, Matamala JM, Carrasco R, Miranda-Merchak A and Feuerhake W: Oxidative stress and pathophysiology of ischemic stroke: Novel therapeutic opportunities. CNS Neurol Disord Drug Targets 12: 698-714, 2013.
6. Shirley R, Ord EN and Work LM: Oxidative stress and the use of antioxidants in stroke. Antioxidants Basel 3: 472-501, 2014.
7. Dias V, Junn E and Mouradian MM: The role of oxidative stress in Parkinson's disease. J Parkinsons Dis 3: 461-491, 2013.
8. Lovell MA and Markesbery WR: Oxidative DNA damage in mild cognitive impairment and late-stage Alzheimer's disease. Nucleic Acids Res 35: 7497-7504, 2007.
9. Khojah HM, Ahmed S, Abdel-Rahman MS and Hamza AB: Reactive oxygen and nitrogen species in patients with rheumatoid arthritis as potential biomarkers for disease activity and the role of antioxidants. Free Radic Biol Med 97: 285-291, 2016.
10. Dröge W: Free radicals in the physiological control of cell function. Physiol Rev 82: 47-95, 2002.
11. Turrens JF: Mitochondrial formation of reactive oxygen species. J Physiol 552: 335-344, 2003.
12. Lee HG and Yang JH: PKC-δ mediates TCDD-induced apoptosis of chondrocyte in ROS-dependent manner. Chemosphere 81: 1039-1044, 2010.
13. Hamann K, Durkes A, Ouyang H, Uchida K, Pond A and Shi R: Critical role of acrolein in secondary injury following ex vivo spinal cord trauma. J Neurochem 107: 712-721, 2008.
14. Hamann K and Shi R: Acrolein scavenging: A potential novel mechanism of attenuating oxidative stress following spinal cord injury. J Neurochem 111: 1348-1356, 2009.
15. Li X, Huo C, Wang Q, Zhang X, Sheng X and Zhang L: Identification of new metabolites of morroniside produced by rat intestinal bacteria and HPLC-PDA analysis of metabolites in vivo. J Pharm Biomed Anal 45: 268-274, 2007.
16. Park CH, Noh JS, Kim JH, Tanaka T, Zhao Q, Matsumoto K, Shibahara N and Yokozawa T: Evaluation of morroniside, iridoid glycoside from Corni Fructus, on diabetes-induced alterations such as oxidative stress, inflammation, and apoptosis in the liver of type 2 diabetic db/db mice. Biol Pharm Bull 34: 1559-1565, 2011.
17. Ai HX, Wang W, Sun FL, Huang WT, An Y and Li L: Morroniside inhibits H_2O_2-induced apoptosis in cultured nerve cells. Zhongguo Zhong Yao Za Zhi 33: 2109-2112, 2008 (In Chinese).
18. Jang SE, Jeong JJ, Hyam SR, Han MJ and Kim DH: Ursolic acid isolated from the seed of Cornus officinalis ameliorates colitis in mice by inhibiting the binding of lipopolysaccharide to Toll-like receptor 4 on macrophages. J Agric Food Chem 62: 9711-9721, 2014.
19. Yu HH, Hur JM, Seo SJ, Moon HD, Kim HJ, Park RK and You YO: Protective effect of ursolic acid from Cornus officinalis on the hydrogen peroxide-induced damage of HEI-OC1 auditory cells. Am J Chin Med 37: 735-746, 2009.
20. Kim SH, Lee MK, Ahn M-J, Lee KY, Kim YC and Sung SH: Efficient method for extraction and simultaneous determination of active constituents in Cornus officinalis by reflux extraction and high performance liquid chromatography with diode array detection. J Liq Chromatogr Relat Technol 32: 822-832, 2009.
21. Li CY, Li L, Li YH, Ai HX and Zhang L: Effects of extract from Cornus officinalis on nitric oxide and NF-kappaB in cortex of cerebral infarction rat model. Zhongguo Zhong Yao Za Zhi 30: 1667-1670, 2005 (In Chinese).
22. Hu JG, Fu SL, Zhang KH, Li Y, Yin L, Lu PH and Xu XM: Differential gene expression in neural stem cells and oligodendrocyte precursor cells: a cDNA microarray analysis. J Neurosci Res 78: 637-646, 2004.
23. Rani V, Deep G, Singh RK, Palle K, Yadav UC and Yadav UC: Oxidative stress and metabolic disorders: Pathogenesis and therapeutic strategies. Life Sci 148: 183-193, 2016.
24. Miranda-Díaz AG, Pazarín-Villaseñor L, Yanowsky-Escatel FG and Andrade-Sierra J: Oxidative stress in fiabetic nephropathy with early chronic kidney disease. J Diabetes Res 2016: 7047238, 2016.
25. Forte M, Conti V, Damato A, Ambrosio M, Puca AA, Sciarretta S, Frati G, Vecchione C and Carrizzo A: Targeting nitric oxide with natural derived compounds as a therapeutic strategy in vascular diseases. Oxid Med Cell Longev 2016: 7364138, 2016.
26. Karpinska A and Gromadzka G: Oxidative stress and natural antioxidant mechanisms: the role in neurodegeneration. From molecular mechanisms to therapeutic strategies. Postepy Higieny i Medycyny Doswiadczalnej (Online) 67: 43-53, 2013.
27. Turkez H, Sozio P, Geyikoglu F, Tatar A, Hacimuftuoglu A and Di Stefano A: Neuroprotective effects of farnesene against hydrogen peroxide-induced neurotoxicity in vitro. Cell Mol Neurobiol 34: 101-111, 2014.
28. Tian LL, Wang XJ, Sun YN, Li CR, Xing YL, Zhao HB, Duan M, Zhou Z and Wang SQ: Salvianolic acid B, an antioxidant from Salvia miltiorrhiza, prevents 6-hydroxydopamine induced apoptosis in SH-SY5Y cells. Int J Biochem Cell Biol 40: 409-422, 2008.
29. Ding X, Wang MY, Yu ZL, Hu W and Cai BC: Studies on separation, appraisal and the biological activity of 5-HMF in Cornus officinalis. Zhongguo Zhong Yao Za Zhi 33: 392-396, 484, 2008 (In Chinese).
30. Jiang X, Nie B, Fu S, Hu J, Yin L, Lin L, Wang X, Lu P and Xu XM: EGb761 protects hydrogen peroxide-induced death of spinal cord neurons through inhibition of intracellular ROS production and modulation of apoptotic regulating genes. J Mol Neurosci 38: 103-113, 2009.
31. Xu H, Shen J, Liu H, Shi Y, Li L and Wei M: Morroniside and loganin extracted from Cornus officinalis have protective effects on rat mesangial cell proliferation exposed to advanced glycation end products by preventing oxidative stress. Can J Physiol Pharmacol 84: 1267-1273, 2006.

32. Hilton JB, White AR and Crouch PJ: Endogenous Cu in the central nervous system fails to satiate the elevated requirement for Cu in a mutant SOD1 mouse model of ALS. Metallomics 8: 1002-1011, 2016.
33. Hwang KA, Hwang YJ and Song J: Antioxidant activities and oxidative stress inhibitory effects of ethanol extracts from *Cornus officinalis* on raw 264.7 cells. BMC Complement Altern Med 16: 196, 2016.
34. Bharat S, Cochran BC, Hsu M, Liu J, Ames BN and Andersen JK: Pretreatment with R-lipoic acid alleviates the effects of GSH depletion in PC12 cells: Implications for Parkinson's disease therapy. Neurotoxicology 23: 479-486, 2002.
35. Deng G, Su JH, Ivins KJ, Van Houten B and Cotman CW: Bcl-2 facilitates recovery from DNA damage after oxidative stress. Exp Neurol 159: 309-318, 1999.
36. Nguyen TT, Stevens MV, Kohr M, Steenbergen C, Sack MN and Murphy E: Cysteine 203 of cyclophilin D is critical for cyclophilin D activation of the mitochondrial permeability transition pore. J Biol Chem 286: 40184-40192, 2011.
37. Del Gaizo Moore V and Letai A: BH3 profiling - measuring integrated function of the mitochondrial apoptotic pathway to predict cell fate decisions. Cancer Lett 332: 202-205, 2013.
38. Li DW, Li JH, Wang YD and Li GR: Atorvastatin protects endothelial colony forming cells against H$_2$O$_2$ induced oxidative damage by regulating the expression of Annexin A2. Mol Med Rep 12: 7941-7948, 2015.
39. Xu H, Luo P, Zhao Y, Zhao M, Yang Y, Chen T, Huo K, Han H and Fei Z: Iduna protects HT22 cells from hydrogen peroxide-induced oxidative stress through interfering poly(ADP-ribose) polymerase-1-induced cell death (parthanatos). Cell Signal 25: 1018-1026, 2013.
40. Neuzil J, Wang XF, Dong LF, Low P and Ralph SJ: Molecular mechanism of 'mitocan'-induced apoptosis in cancer cells epitomizes the multiple roles of reactive oxygen species and Bcl-2 family proteins. FEBS Lett 580: 5125-5129, 2006.